International Symposium
On Turbulence and Shear Flow
Phenomena (TSFP-8)
August 28 - 30, 2013 Poitiers, France

UNSTEADY SEPARATION CONTROL USING SPATIALLY-COMPACT PULSED ACTUATION

George T. K. Woo
George W. Woodruff School of Mechanical Engineering
Georgia Institute of Technology
771 Ferst Drive NW, Atlanta, Georgia 30332, USA
gtkwoo@gatech.edu

Ari Glezer
George W. Woodruff School of Mechanical Engineering
Georgia Institute of Technology
771 Ferst Drive NW, Atlanta, Georgia 30332, USA
ari.glezer@me.gatech.edu

ABSTRACT

The dynamics of controlled 3-D transitory attachment of stalled flow over a static and dynamically pitching 2-D airfoil is investigated in wind tunnel experiments. Pulsed actuation is effected over a spanwise fraction of the separated domain on a time scale that is an order of magnitude shorter than the characteristic convective time scale using surface-integrated pulsed, combustion-driven actuator jets. The dynamics of vorticity concentrations over the airfoil and in its near wake is computed from high-resolution PIV measurements of the flow field that are obtained phase-locked to the actuation in multiple cross-stream planes. The present measurements show that transitory attachment spreads towards the outboard, unactuated flow domains and far exceeds the spanwise width of the actuator. The attachment is accompanied by the formation of 3-D vortical structures that are advected and shed into the near wake. It is shown that coupling of the pulsed actuation to the airfoil's motion enhances the control authority of 3-D unsteady separation and can significantly mitigate the adverse effects of dynamic stall on the unsteady lift and pitching moment.

EXPERIMENTAL SETUP AND PROCEDURES

Transitory, 3-D attachment induced by pulsed actuation is investigated experimentally over a 2-D NACA-4415 airfoil ($c = 457$ mm, $S \approx 890$ mm). The model is partitioned into three sections by streamwise acrylic fences that are installed symmetrically about the airfoil's center plane $z = 0$ (Figure 1a). The center segment is instrumented with a spanwise array of seven, individually addressable combustion-based (COMPACT) jet actuators located at $x/c = 0.15$ symmetrically about $z = 0$ within the center segment while the two outboard segments are unactuated. In the present experiments, $S_c = S$ and the seven actuators are triggered synchronously producing high velocity pulsed jets (span $S_a \approx 0.21 S_c$) that emanate from the airfoil upper surface via a rectangular orifice (0.19 x 20 mm).

The airfoil model is mounted on a 2-DOF (pitch and plunge) traverse. The time-dependent lift force, $C_L(t)$, and pitching moment, $C_M(t)$, are measured independently using built-in load cells and a torque sensor. For the dynamic experiments, the model is oscillating about its pitch axis defined by $\alpha(t) = \alpha_0 + \alpha_P \sin(\omega t)$ where α_0 is the nominal average angle of attack, α_P is the oscillation amplitude, and $k = \omega c/2U_\infty$ is the reduced frequency. Figure 1b shows a schematic representation of the oscillatory motion and actuation timing.

The experiments are conducted in an open-return wind tunnel with a test section measuring approximately 0.9 x 0.9 m. The free stream velocity is $U_\infty = 20$ m/s ($Re_c = 570{,}000$) and the convective time scale of the flow over the airfoil is $T_{conv} \approx 25$ msec. The flow about the airfoil and in its near wake is characterized using phase-locked, high-speed particle image velocimetry (PIV) in several cross-stream planes (constant z) using two synchronized CMOS cameras (1280 x 800 pixels). The flow is seeded with micron-size fog particles and is illuminated using a double-pulse Nd-YLF laser. Sets of PIV images are captured at a sequence of predetermined time delays relative to the actuation trigger and model trajectory.

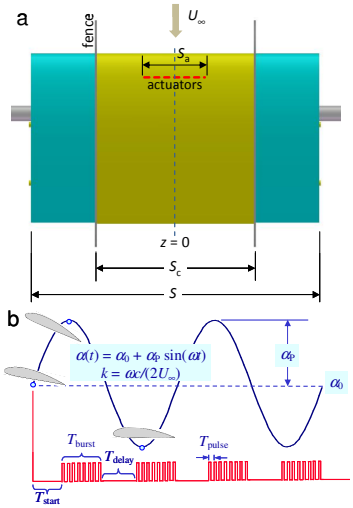

Figure 1. The airfoil model with flow partitions and integrated combustion actuator array (a). The timing of model motion and actuation (b). For the present experiments, $S_c = S$.

TRANSITORY CONTROL OF SEPARATION

The present work builds on the earlier investigations of the transient response of a nominally 2-D separated flow to *bounded* 2-D pulsed actuation on static and pitching airfoils by Brzozowski et al. (2006 and 2010), Woo et al. (2008 and 2009), and Woo and Glezer (2010 and 2011). These investigations demonstrated that a single actuation pulse can lead to brief, partial collapse of the separated flow domain, coupled with a momentary increase in circulation.

Spatially-Compact Actuation on Static Airfoil

Previous investigations, by Woo and Glezer (2013), of the three-dimensional flow interactions that are induced over the center section of the stalled static airfoil at $\alpha = 19°$ following single pulse actuation demonstrated that the actuation resulted in the collapse of the spanwise center of the separated flow downstream of the actuator array. In these investigations, with a reduced center section span ($S_c \approx 0.52S$ where the baseline separation is approximately 2-D) and using only the center three actuator jets ($S_a \approx 0.17S_c$), the spanwise domain of influence of the actuation was somewhat wider than the spanwise extent of the active actuator array. This was manifested by a significant reduction in the cross-stream width of the wake where Δy_{wake} (for $u \leq U_\infty$), as measured at $0.1c$ downstream of the trailing edge, was reduced relative to baseline by 45% and 28% at $z = 0$ and $0.5S_a$, respectively, at $2.7T_{conv}$ after the onset of actuation. The near wake also exhibited strong spanwise gradients of the streamwise velocity within the transition region between the partially-attached and separated flow domains suggesting the presence of cross-stream vorticity ostensibly owing to tilting of spanwise vorticity concentrations. Relaxation occurred within $10T_{conv}$.

Figure 2 shows perspective view of phase-averaged concentrations of spanwise vorticity following single pulse actuation in the cross-stream planes $z/c = 0$, 0.17, 0.27, and 0.39 (for clarity, the data are mirrored about center-span) where the cross-stream and streamwise extent of the data fields are $-0.55 < y/c < 0.25$ and $0.24 < x/c < 1.5$. To further elucidate the features of the 3-D flow structures, interpolated iso-surfaces of vorticity concentrations are viewed in two different orientations in Figure 3. The 7-actuator array is shown as block arrows on the airfoil in Figures 2 and 3.

The baseline flow field (Figures 2a and 3a) immediately following the onset of the actuation shows minor 3-D spanwise variations including a decrease in the cross stream extent of the separation with z. The center three planes ($-0.17 \leq z/c \leq 0.17$) encompass the full width of the actuator array ($S_a \approx 0.2S_c \approx 0.34c$), and the onset of the severing of the separating shear layer and the formation of a CW vortex is visible in these planes at $t = 0.4T_{conv}$ (Figure 2b) near $x/c = \approx 0.4$. By $0.56T_{conv}$ (Figure 2c), the transitory effects induced by the actuation spread beyond the actuated region as manifested by the formation of a CW vortex at $z = 0.27c$ ($x/c \approx 0.5$). It is noteworthy that the data in the plane $z/c = 0.39$ show little or no evidence of the rollup of this vortex which is also evident in the vorticity iso-surfaces in Figure 3b. The rollup of this vortex progresses in the span farther downstream (at $t = 0.72T_{conv}$, Figures 2d and 3c) as the CW vortex is advected towards the trailing edge (Figures 2e-g and 3d-e), indicating that the instability that leads to the rollup (and the following attachment of the upstream surface vorticity layer) spreads along the span of the flow into the interface domain between the attached and separated flows. This spanwise spreading might be similar to the inviscid instability that leads to the rollup of vortices within nominally plane shear layers. The rate of spanwise spreading is clearly dominated by the advection speed or celerity of the "primary" CW vortex that is "seeded" by the

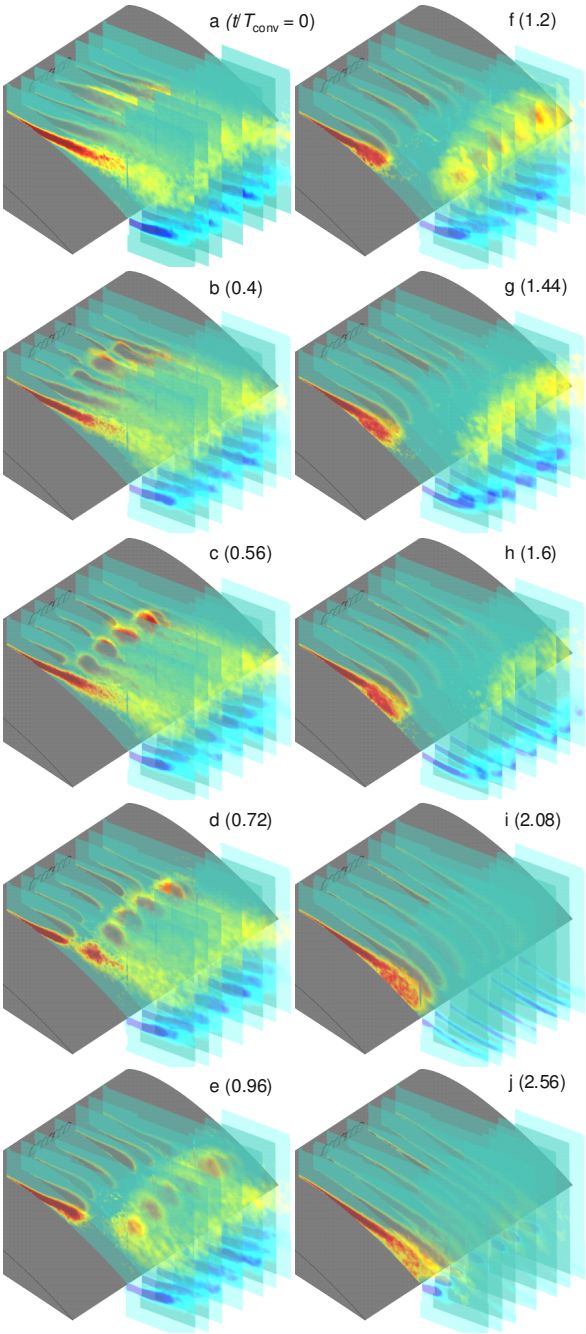

Figure 2. Phase-averaged vorticity maps in the cross stream planes $z/c = 0$, ±0.17, ±0.27 and ±0.39 at $\alpha = 19°$ following single unbounded 3-D ($S_a \approx 0.2S$ and $S_c = S$) pulsed actuation applied at $t = 0$: $t/T_{conv} = 0$ (a), 0.4 (b), 0.56 (c), 0.72 (d), 0.96 (e), 1.2 (f), 1.44 (g), 1.6 (h), 2.08 (i), and 2.56 (j) with actuation extent shown as arrows.

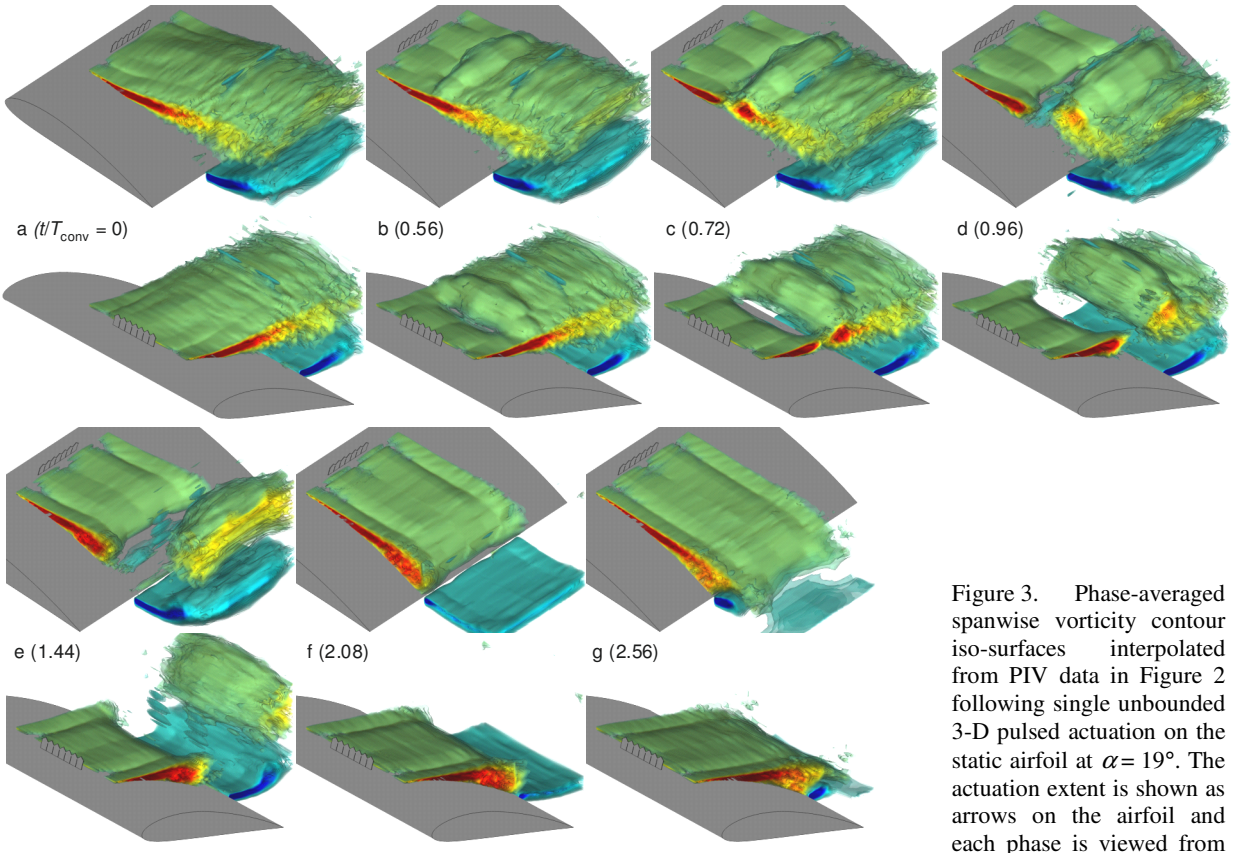

Figure 3. Phase-averaged spanwise vorticity contour iso-surfaces interpolated from PIV data in Figure 2 following single unbounded 3-D pulsed actuation on the static airfoil at $\alpha = 19°$. The actuation extent is shown as arrows on the airfoil and each phase is viewed from

actuation, and is terminated when the vortex is shed into the near wake. Since the formation of this vortex induces the attachment of the surface vorticity layer upstream, the spanwise spreading rate ultimately affects the spanwise extent of attached flow.

The data in Figure 2 show that the attachment domain of the upstream surface vorticity layer is spanwise non-uniform because of the spanwise delay in the rollup of the CW vortex. By $t = 2.56T_{conv}$ (Figures 2f-j and 3e-g), the flow is attached in all the z-planes, confirming that the effects of actuation extend significantly beyond the actively-actuated domain. Since the advection velocity of the attached flow is clearly lower than the characteristic velocity of the separated shear layer, the attached flow near center span is advected slower than near the spanwise edged of the interface domain. For this reason, the nominally-attached vorticity layer in the outboard edges of the interface is thicker than near the centerline. The iso-surfaces in Figures 3b-e clearly show the interface between the attached and separated flow domains immediately following the shedding of the CW vorticity concentration. The present measurements do not resolve the streamwise and cross stream vorticity components and therefore the details of the vortical connection between the interface edges and the shed CW vortex remain obscure, but it seems reasonable to conjecture that the shedding gives rise to streamwise vortical structures similar to tip vortices. Finally, coupled with the spanwise evolution of the CW vorticity concentrations from the suction surface, there are also significant spanwise variations in concentrations of the CCW vorticity in the near wake (Figures 2f-j and 3e-g) as the global circulation is effectively modulated by the actuation.

Timed-Interactions of Unsteady Separation Control

The receptivity of the separated flow to pulsed actuation is explored by coupling the actuation to time-periodic separation on an airfoil that is dynamically pitching beyond its stall margins. An important parameter of the coupling is the timing of the (single) actuation pulse (T_{start}) relative to the pitch cycle that enables variation of the pulse timing relative to the onset of separation (Woo and Glezer, 2013). The pitch cycle period is $T_P = 625$ ms, $\alpha_o = 14°$, $\alpha_P = 4°$ and $k = 0.115$ (the airfoil pitches up through 14° at $t = 0$). The phase-averaged lift and pitching moment for the baseline airfoil and in the presence of pulse actuation for a range of T_{start} are shown in Figures 4a-h, and 4i-p, respectively. The variation of integral measures of the global lift and pitching moment with T_{start} are shown in Figures 5a-c.

As a result of the pitch, separation of the baseline flow (gray dashed traces) occurs at higher α such that the unsteady lift increases beyond the corresponding static C_L and the onset of dynamic stall occurs near the maximum angle on the upstroke with significant loss in lift that is associated with the shedding of the dynamic stall vortex and large-scale separation during the downstroke. Undesirable effects of pitch instability or "negative damping" (e.g. Carta, 1967, McCroskey, 1982, and Carr, 1988) that are associated with the changes in aerodynamic moment on the airfoil can induce vibrations and lead to possible structural damage. As shown in Figure 4i, the baseline airfoil

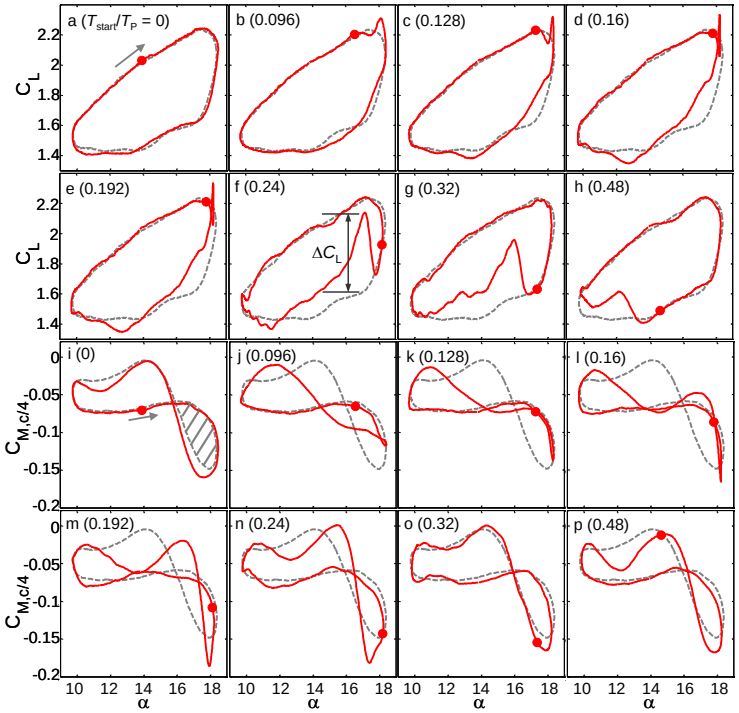

Figure 4. Dynamic lift, C_L, (a-h) and pitching moment, $C_{M,c/4}$, (i-p) curves showing the effects of unbounded 3-D ($S_a \approx 0.2S$ and $S_c = S$) single-pulse actuation (●) applied at T_{start}/T_P= 0 (a,i), 0.096 (b,j), 0.128 (c,k), 0.16 (d,l), 0.192 (e,m), 0.24 (f,n), 0.32 (g,o) and 0.48 (h,p) during airfoil pitching cycle (T_P = 625 ms and k = 0.115). The corresponding baseline traces are shown in dashed curves and the directions of the phase plots are indicated by an arrow (a, i).

experiences negative damping for $\alpha > 15.5°$ as $C_{M,c/4}$ which is nearly time-invariant for the majority of the up-stroke increases rapidly in magnitude until the early stages of the down-stroke. The negative pitching moment subsequently decreases in magnitude as the airfoil continues to pitch down through $\alpha < 15.5°$, and the reversal is manifested in a CW loop of $C_{M,c/4}(\alpha)$ as shaded in Figure 4i.

When the actuation pulse is applied on the upstroke before the onset of dynamic stall ($0 \le T_{start}/T_P \le 0.192$, Figures 4a-e), lift is increased beyond the baseline values immediately following the actuation and remains above the baseline values for an extended fraction of the down-stroke. As the actuation pulse is delayed until the down-stroke (e.g., T_{start}/T_P = 0.24 and 0.32 in Figures 4f and g), the unsteady global lift increases significantly ($\Delta C_L \approx 0.55$ for T_{start}/T_P = 0.24) over a short time (~$0.05T_P$) and relaxes within $0.24T_P$ thereafter. The enhanced receptivity to actuation with increasing T_{start} is shown in Figures 5a and b in terms of the reduction in the degree of hysteresis (L^*) by almost 30% for $0.2 < T_{start}/T_P < 0.4$, and the increase in cycle-averaged lift (L^*_{cycle}) which reaches a maximum (about 3%) when $T_{start} \approx 0.24T_P$.

The actuation also has significant effects on the pitching moment. For $0 < T_{start}/T_P < 0.16$ (Figures 4i-l), the extent of negative damping is reduced as manifested by the reduction in the hysteresis loop over the large pitch angles (e.g., T_{start}/T_P = 0.128 and 0.16 in Figures 4k and l, respectively). Figure 5c shows that pulsed actuation can effectively control the cumulative pitching moment where the change in $\int C_{M,c/4}dt$ is maximum when the pulsed jets are triggered at T_{start}/T_P = 0.128, coinciding with the largest suppression of negative damping as shown in Figure 4k. For

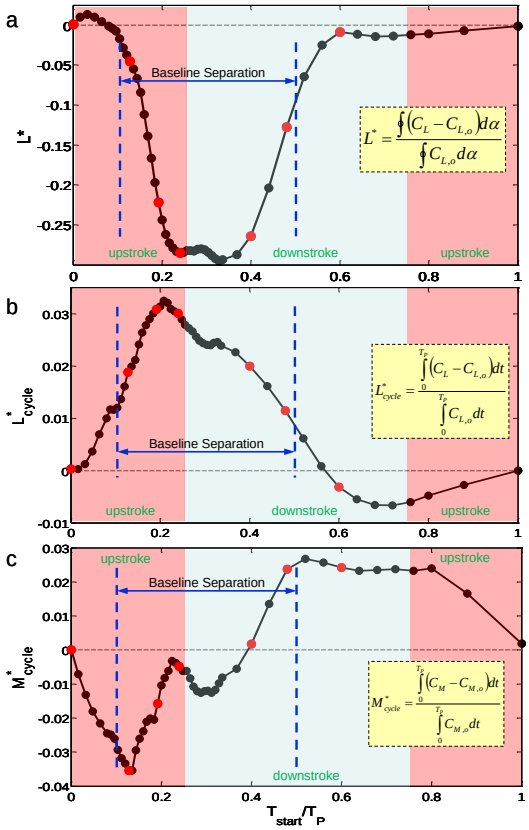

Figure 5. Phase- (a) and time-integral (b, c) of the unsteady lift (a and b) and pitching moment (c) for single-pulse actuation with different T_{start} (●) in the pitching cycle (T_P = 625 ms and k = 0.115). The corresponding actuation cases in Figure 4 are included (●).

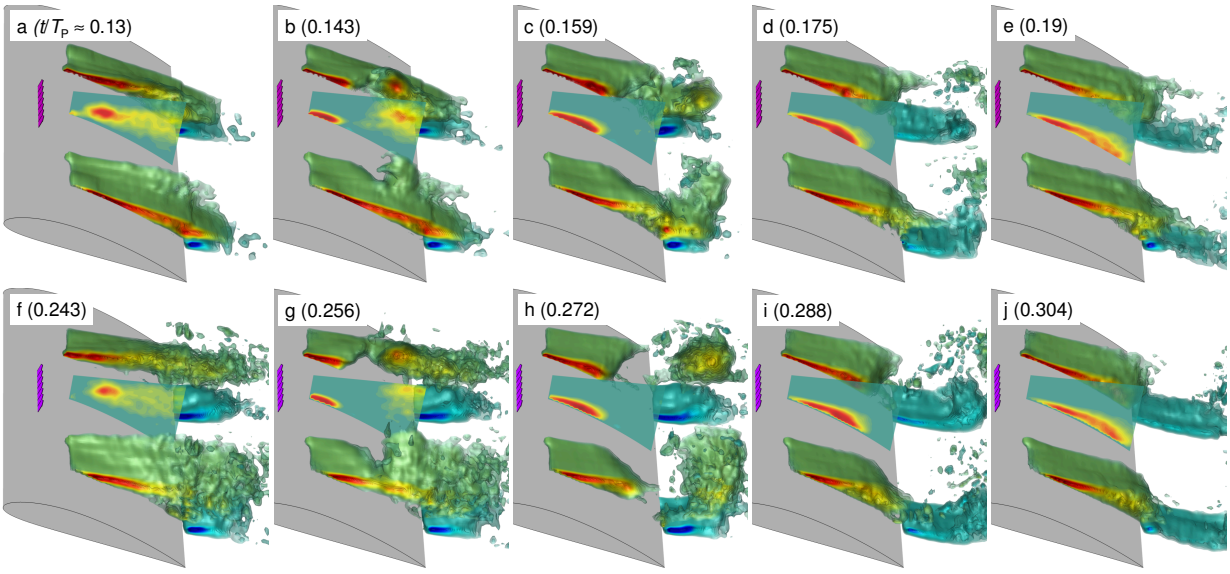

Figure 6. Phase-averaged spanwise vorticity maps in the centerplane $z = 0$ following single unbounded 3-D ($S_a \approx 0.2S$ and $S_c = S$) pulsed actuation applied at $t/T_P = 0.128$ (a-e) and 0.24 (f-j) when the airfoil is undergoing periodic oscillations in pitch ($T_P = 625$ ms and $k = 0.115$). The corresponding iso-surface contours of the spanwise vorticity interpolated from PIV data at $z/c = \pm 0.33$, ± 0.38, ± 0.44, ± 0.49 and ± 0.55 are included, and the 7-actuator array is shown as arrows on the airfoil.

$0 \leq T_{start}/T_P \leq 0.128$, as the airfoil pitches up through the high angles but with a decreasing positive pitch rate, Figure 5c shows improved control authority in effecting pitch stability. The control authority of the single pulse diminishes as the actuation delay increases (e.g., $T_{start} = 0.48T_P$ in Figure 4h). This is in agreement with Figures 5a and b where L^* and L^*_{cycle} returns to baseline for $0.4 < T_{start}/T_P < 0.6$ and $0.24 < T_{start}/T_P < 0.6$, respectively. Thereafter, the effectiveness of actuation is negligible as the flow over the airfoil at low α is attached.

The differences in the flow response (in the cross-stream planes $z/c = 0$, 0.33, 0.38, 0.44, 0.49, and 0.55) that is associated with the aerodynamic performance of the airfoil for actuation applied at $T_{start}/T_P = 0.128$ and 0.24 (Figures 4c, k, and f, n respectively, and Figure 5) are shown in Figures 6a-e and 6f-j, respectively. The spanwise vorticity concentrations at $z = 0$ are shown only for the flow domain downstream of the actuators above the airfoil while to elucidate the features of the 3-D flow structures over the unactuated region ($0.33 \leq z/c \leq 0.55$), iso-surfaces of vorticity concentrations over the airfoil and in the near wake interpolated from the PIV data are shown mirrored about the centerplane. Figures 6a and f show the flow field (during the up- and down-strokes at $\alpha \sim 17.3°$, respectively) at a short time following actuation prior to any measurable actuation effects in the near wake. Aside from the difference in motion between these two states, they also differ by the cross-stream extent of the separation domain, which also affects the receptivity and response of the flow. The cross-stream width of the near wake (for $u \leq U_\infty$), Δy_{wake}, is measured at $0.2c$ downstream of the trailing edge. On the up-stroke as the salient unsteady separation develops initially over the center segment of the airfoil (Figure 6a), Δy_{wake} decreases rapidly towards the outboard domains of the flow (e.g., from $\Delta y_{wake} \approx 0.34c$ at $z = 0$ to $0.19c$ at $z = 0.38c$) compared to on the down-stroke where the larger separation (at $z = 0$ and $0.33 \leq z/c \leq 0.55$ in Figure 6f) shows only minor 3-D spanwise variations ($\Delta y_{wake} \approx 0.46c$ and $0.35c$ at the corresponding locations $z = 0$ and $0.38c$).

For both instances, the attachment is clearly evident at the centerspan. However, the actuation-induced CW vortex remains somewhat closer to the airfoil as it advects downstream for $T_{start}/T_P = 0.128$ and contains higher circulation (compare the relative cross-stream locations and the limited spanwise spreading of the vortical structures in Figures 6b and c with the amplified motion of the corresponding larger structures in Figures 6g and h). There is also noticeably higher concentrations of CW vorticity in the boundary layer for $T_{start}/T_P = 0.128$ (Figures 6b-e) compared to $T_{start}/T_P = 0.24$ (Figures 6g-j) that is coupled with enhanced accumulation rate during the upstroke and therefore results in the higher transitory C_L. However, this change is brief and only delays the onset of stall (Figure 4c). During this time, by reattaching the partially-separated flow as the airfoil continues to pitch up albeit at a reduced rate, the transitory changes in the pressure distribution that corresponds to the (spanwise and temporal) modulations of the spanwise vorticity above the airfoil significantly suppress the onset of negative damping (Figure 4k). Similar pressure transients are also observed by Woo and Glezer (2013) with 2-D bounded actuation applied to a nominally 2-D unsteady separated flow.

In contrast, when actuation is applied at $T_{start}/T_P = 0.24$ in the presence of extensive separation, albeit the effective reattachment of the flow on the down-stroke, the actuation pulse is unable to reverse the onset of negative damping (Figure 4n) that is already induced by the corresponding 3-D pressure distributions during the large-scale separation. However, the attached boundary layer (Figures 6g-j), does not separate again, and when coupled to the down-stroke of the airfoil results in a prolonged, larger increase in C_L above baseline (Figure 4f compared to Figure 4c). The attachment in Figures 6g-j show increased spanwise 3-D variations toward the edges of the PIV measurement domain where it

seems reasonable to conjecture that transitory streamwise vortical structures are formed near the flow interface between the actuated and unactuated regions for $T_{start} = 0.24T_P$.

CONCLUSIONS

Transitory, 3-D control of the flow within the separated flow domain over a stationary and dynamically-pitching 2-D airfoil is investigated in wind tunnel experiments using spatially-compact (21% span) pulsed actuation by an array of momentary jets having a characteristic time scale that is an order of magnitude shorter than the convective time scale of the flow.

High resolution PIV measurements of the stalled flow over the stationary airfoil show that the separated flow is highly susceptible to 3-D, single pulse actuation. The actuation leads to spanwise-localized severing of the separating shear layer and consequently to the formation and rollup of large-scale *free* vortex that is advected downstream while inducing attachment of a surface vorticity layer within a spanwise-limited domain. While the detached vortex is advected downstream, the severing and rollup are extended in the spanwise direction well beyond the edges of the actuator, and concomitantly lead to spanwise spreading of the attached surface vorticity layer upstream, thereby extending the attached flow domain while the outboard segments of the stalled flow remain separated. The rate of spanwise and streamwise spreading are clearly dominated by the advection speed or celerity of the detached CW vortex that is first "seeded" by the actuation, and is terminated when the vortex is finally shed into the near wake.

The receptivity of the separated flow to the 3-D pulsed actuation is exploited for controlling the time-periodic separation on an airfoil that dynamically-pitches beyond its stall margins. Specific emphasis is placed on the phase of the (single) actuation pulse relative to the airfoil motion, and it is shown that the control authority can be extended by deliberate coupling of the pulsed actuation to the airfoil's motion to take advantage of controlled temporal interactions with unsteady 3-D separation. Within some range, synchronizing the onset of the actuation to the pitching cycle can significantly mitigate the effects of dynamic stall and improve the unsteady aerodynamic lift and pitching moment. The magnitude of the time-dependent lift hysteresis owing to the onset of dynamic stall is reduced along with an increase in the cycle-averaged lift. Furthermore, it is shown that single-pulse actuation can effectively reduce the extent of negative damping during the pitching cycle. The flow dynamics of the transitory attachment over the pitching airfoil induced by single-pulsed actuation at two different delays indicate that with the increased receptivity of the unsteady separation to spatially-compact pulsed actuation, the improvements in the unsteady lift or the reduction in negative damping in the pitching moment result from 3-D flow features that evolve over the airfoil and are enhanced by its motion but differ with the upstroke and downstroke motions. Enhanced accumulation of vorticity during the upstroke results in the higher transitory C_L at high angles of attack as the onset of stall is briefly delayed, while actuation during the downstroke following dynamic stall results in a prolonged, larger increase in C_L above baseline due to attachment of the large-scale separation.

REFERENCES

Brzozowski, D., Woo., G. T. K., Culp, J., and Glezer, A., "Transient Separation Control using Pulse-Combustion Actuation," AIAA J., 48, 2482-2490, 2010.

Brzozowski, D., and Glezer, A., "Transient Separation Control Using Pulse-Combustion Actuation," AIAA Paper 2006-3024, 2006.

Carr, L. W., "Progress in analysis and prediction of dynamic stall," J. Aircraft, 25(1):6-17, 1988.

Carta, O. F., "Unsteady Normal Force on an Airfoil in a Periodically Stalled Inlet Flow," AIAA J., 4(5): 416-421, 1967.

McCroskey, W. J., "Unsteady Airfoils", Ann. Rev. of Fluid Mechanics, 14, 285-311, 1982.

Woo, G. T. K., Crittenden, T., and Glezer, A., "Transitory Control of a Pitching Airfoil using Pulse Combustion Actuation," AIAA Paper 08-4324, 2008.

Woo, G. T. K., Crittenden, T., and Glezer, A., "Transitory Separation Control over a Stalled Airfoil," AIAA Paper 09-4281, 2009.

Woo, G. T. K., and Glezer, A., "Transient Control of Separating Flow over a Dynamically-Pitching Airfoil," AIAA Paper 2010-861, 2010.

Woo, G. T. K., Crittenden, T., and Glezer, A., "Transitory Control of Dynamic Stall on a Moving Airfoil," AIAA Paper 2011-0489, 2011.

Woo, G. T. K., and Glezer, A., "Three-Dimensional Transitory Control of Flow Separation over a 2-D Airfoil," AIAA Paper 2013-1116, 2013.

Woo, G. T. K., and Glezer, A., "Controlled Transitory Stall on a Pitching Airfoil using Pulsed Actuation," Exp. Fluids, 54:1507, 2013. doi: 10.1007/s00348-013-1507-5